ARTICLE

Electron Injection from Colloidal PbS Quantum Dots into Titanium Dioxide Nanoparticles

Byung-Ryool Hyun,[†,*] Yu-Wu. Zhong,[‡] Adam C. Bartnik,[†] Liangfeng Sun,[†] Hector D. Abruña,[‡] Frank W. Wise,[†] Jason D. Goodreau,[§] James R. Matthews,[§] Thomas M. Leslie,[§] and Nicholas F. Borrelli[§]

[†]Department of Applied Physics and [‡]Department of Chemistry and Chemical Biology, Cornell University, Ithaca, New York 14850, and [§]Corning, Inc., Corning, New York 14831

ABSTRACT Injection of photoexcited electrons from colloidal PbS quantum dots into TiO_2 nanoparticles is investigated. The electron affinity and ionization potential of PbS quantum dots, inferred from cyclic voltammetry measurements, show strong size dependence due to quantum confinement. On the basis of the measured energy levels, photoexcited electrons should transfer efficiently from the quantum dots into TiO_2 only for quantum-dot diameter below ~4.3 nm. Continuous-wave fluorescence spectra and fluorescence transients of PbS quantum dots coupled to titanium dioxide nanoparticles are consistent with electron transfer for small quantum dots. The measured electron transfer time is surprisingly slow (~100 ns), and implications of this for future photovoltaics will be discussed. Initial results obtained from solar cells sensitized with PbS quantum dots are presented.

KEYWORDS: PbS QDs · near-infrared · electron transfer time · titanium dioxide · solar cells · cyclic voltammetry · **k · P** theory · electron affinity · fluorescence lifetime

Semiconductor nanocrystals or quantum dots (QDs) have attracted research interest for the development of solar cell devices due to their unique features. These include size-dependent optical absorption spectra, large extinction coefficients, and extended photostability, which underlie efficient harvesting of light energy. Their nanoscale sizes are compatible with nanostructured electrode materials. QDs also offer the intriguing possibility of overcoming the ordinary thermodynamic limits of solar energy conversion if multiple[1,2] or hot[3] charge carriers can be extracted. A variety of configurations, such as QD superlattice arrays,[4] QD-sensitized cells, and QDs dispersed in organic semiconductor polymers,[5] have been considered as next-generation photovoltaic devices, with over 80% solar conversion efficiency expected in tandem solar cells.[6]

A typical strategy to construct solar cells based on QDs is to use semiconductor QDs as the sensitizer in porous metal oxide nanostructure films, in analogy to dye-sensitized films.[7] Sensitization of mesoporous TiO_2 and SnO_2 films using CdS,[8−11] CdSe,[12,13] InP,[14] InAs,[15] and PbS[16−18] QDs has been reported, and charge transfer from the QDs into the TiO_2 and SnO_2 films has been demonstrated *via* several types of measurements. Among the various QD materials, PbS and PbSe are good candidates for solar cells, because they can be made to overlap the solar spectrum optimally. By controlling their size, the absorption wavelength of the first exciton peak can easily be extended into the infrared.[19] The occurrence and mechanism of carrier multiplication in QDs are currently subjects of intense debate and research. However, the first, the most consistent, and the most dramatic indications of carrier multiplication have been obtained with PbS and PbSe QDs. Photon-to-exciton conversion efficiency up to 700% has been claimed.[20]

Hoyer and co-workers studied a solar cell structure made by *in situ* growth of PbS QDs in a porous TiO_2 film,[16−18] and Plass *et al.*[17] later investigated electron transfer in the same structure. Although the successful incorporation of the QDs in the mesoporous TiO_2 is encouraging, this approach is not optimal. As evidenced by the featureless absorption spectra, the QD size distribution was broad. The consequent variation in the energy level alignment could lead to an energy barrier, rather than a favorable energetic pathway, to electrons in a significant fraction of the QDs. It is also likely that the QDs synthesized *in situ* do not have the high-quality surfaces available with the best modern colloidal syntheses. The resulting surface states tend to be efficient traps for photoexcited charge carriers and thus interfere with the efficient extraction of charge from the QDs. The energy conversion efficiency obtained through the *in situ* growth was fairly low, perhaps as a

*Address correspondence to bh73@cornell.edu.

Received for review June 2, 2008 and accepted October 22, 2008.

Published online October 31, 2008. 10.1021/nn800336b CCC: $40.75

consequence of the issues above. Independent characterization of the QDs is obviously difficult when they are grown *in situ*.

Recently developed colloidal syntheses produce PbS[21,22] and PbSe[23] QDs with monodisperse size distributions, clear and discrete optical transitions, and high fluorescence quantum yield. Size control allows selection of the QDs that optimize the energy-level alignment with the various metal-oxide electrode materials. In addition, separate and thorough characterization of the semiconductor QDs and the nanoscale metal oxide facilitates understanding of the composite material.

Here, we report a study of electron transport from colloidal PbS QDs to titanium dioxide nanoparticles. This work is motivated by the potential of the lead-salt QDs for sensitizing solar cells. The relevant energy levels of PbS QDs are obtained from cyclic voltammetry (CV) measurements together with the known electronic states of the QDs. The inferred energies agree well with a simple model of the electron affinity and ionization potential of semiconductor nanocrystal. PbS QDs are attached to TiO_2 nanoparticles with a bifunctional linker molecule with thiol groups on one end and carboxylic groups on the other. Continuous-wave and time-resolved fluorescence spectra exhibit strong quenching for appropriate QD sizes, and this is clear evidence of electron transfer from the QDs to the TiO_2 nanoparticles. The fluorescence transients, along with femtosecond transient absorption measurements, indicate that electron transfer is somewhat slower than expected. The implications of these results for solar energy conversion will be discussed.

RESULTS AND DISCUSSION

For Gratzel-type solar cells sensitized by semiconductor QDs, carrier injection from the QDs to the metal oxide electrodes is required. Since TiO_2 is an *n*-type semiconductor, photoexcited electrons should have energy above the edge of the conduction band of the TiO_2 nanoparticles. Colloidal PbS QDs were synthesized with energy gaps between 0.8 and 1.8 eV by literature procedures[21,22] that build on Murray's approach.[23] Cyclic voltammetry was performed on the QDs, with the results summarized in Table 1. For each size of QD, the lowest unoccupied molecular orbital (LUMO) is determined from the CV data assuming that the energy level of Ag/AgCl in saturated NaCl is 4.7 eV below the vacuum level (see the Supporting Information). The highest occupied level is then obtained by subtracting the measured QD energy gap, ignoring any corrections due to the binding energy of the exciton. This is justified because those corrections are on the order of a few percent in the lead-salts,[24] which is the same order as the precision of our measurements. The resulting energies are shown in Figure 1 (red circles) along with analogous data for PbSe QDs (blue circles) reported by Jiang *et al*. in ref 25.

TABLE 1. LUMO and HOMO Levels of the PbS QDs

entry	abs max (nm)[a]	diameter (nm)	$E_{p,c}$[b] (V)	LUMO[c] (eV)	HOMO[d] (eV)	E_g[e] (eV)
1	730	2.9	−1.24	−3.5	−5.2	1.70
2	870	3.4	−0.96	−3.7	−5.1	1.43
3	1055	4.0	−0.76	−3.9	−5.1	1.18
4	1245	4.8	−0.71	−4.0	−5.0	1.00
5	1440	5.7	−0.58	−4.1	−5.0	0.86
6	1690	6.6	−0.36	−4.2	−5.0	0.73

[a]First exciton absorption maximum. [b]First reduction peak in the initial cathodic scan of CV (vs Ag/AgCl in saturated NaCl). [c]Deduced from CV. [d]Extracted from the absorption spectrum of the PbS QDs. [e]The energy gap is taken as the energy of the lowest exciton absorption peak.

Theoretical modeling of the relevant energy levels is based on quantum confinement of charge carriers together with dielectric effects. A 4-band model based on a $\mathbf{k}\cdot\mathbf{P}$ Hamiltonian[24] accounts for the optical spectra of PbS and PbSe QDs reasonably well. By itself, such a model cannot determine the energy levels relative to vacuum. Brus proposed a way to extend effective-mass models to account for the electrostatic effects of a charged dielectric sphere and penetration of the carrier wave function into the host.[26] To the lowest order, this model depends only on the dielectric constant of the QDs and it yields a simple additive correction to the $\mathbf{k}\cdot\mathbf{P}$ energy levels:

$$E_{QD,vac} = E_{\mathbf{k}\bullet\mathbf{p}} + \left(1 - \frac{1}{\varepsilon_{QD}}\right)\frac{e^2}{2R} + \chi_{bulk} \qquad (1)$$

$E_{QD,vac}$ is the energy level relative to vacuum, $E_{k\bullet p}$ is the energy level from the $\mathbf{k}\cdot\mathbf{P}$ calculation (with the zero of energy taken as the conduction band edge of the bulk crystal), ε_{QD} is the dielectric constant of the QD, R is the radius of the QD, and χ_{bulk} is the electron affin-

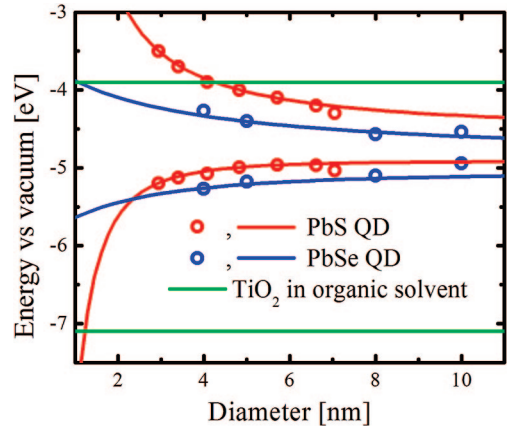

Figure 1. Energy levels of various sizes of PbS and PbSe QDs and TiO_2 nanoparticles. The experimental levels of the PbS QDs (red circles) are obtained from absorption spectra and CV measurements. The energy levels of the PbSe QDs (blue circles) are from ref . The calculated energy levels for PbS and PbSe QDs are represented by solid red and blue lines, respectively. Solid green lines represent electron affinity and ionization potential of TiO_2 nanoparticles in organic solvent.

ity of the bulk semiconductor. The bulk electron affinity was allowed to vary as a fit parameter. However, the inferred values agree well with literature values (below). This model accounts well for the energies of PbS QDs (red line in Figure 1). The same procedure does not account as well for the energies of PbSe QDs. This might be expected, given that the $\mathbf{k}\cdot\mathbf{P}$ model is not as accurate quantitatively in the case of PbSe. The energy levels of PbSe QDs were calculated with the $\mathbf{k}\cdot\mathbf{P}$ model, but the QD diameter associated with each wave function was determined from experimental values.[27] This can be viewed as an empirical correction to the calculation, and the results are also shown in Figure 1. The inferred electron affinity of PbS is −4.55 eV, close to the literature value of −4.6 eV.[28,29] Fitting the data for PbSe QDs yields the value of −4.68 eV for the electron affinity, close to the value of −4.7 eV[30] inferred from a calculation of the PbS−PbSe band offset.

For dye-sensitized solar cells, nonaqueous solvents are preferred as they offer a wider range of electrochemical stability and greater solubility for electrolytic solutes. The electron affinity (−3.9 eV) and ionization potential (−7.1 eV) of TiO_2 nanoparticles[31] in organic solvents are displayed as the solid green lines in Figure 1. From these results, we would expect that efficient electron transfer from PbS QDs to TiO_2 will only occur for QD diameters below ~4.3 nm. PbSe QDs would have to be smaller than 1 nm, at which point the structure will not have a crystal lattice and is more properly viewed as a cluster. In any case, electron transfer from PbSe nanocrystals to TiO_2 is not energetically favorable under the conditions considered here.

We first investigated the properties of TiO_2 nanoparticles linked to 4.8 nm PbS QDs, for which electron transfer is not expected. The optical absorption spectrum of the QD-TiO2 composite is essentially identical to that of the QDs alone (Figure 2a). The absorbance decreases slightly at the lowest exciton peak and increases slightly at wavelengths below 1100 nm. As seen in Figure 2b, the emission peak of the PbS−TiO_2 composite is slightly broader and lower than that of the PbS QDs, but the area is approximately unchanged. The lack of emission quenching of the PbS QD-TiO_2 composites can be explained by the relationship of the reduction potential of the thiol ligands and the valence band edge position of PbS QDs. It is well-known that aliphatic thiol ligands lead to fluorescence quenching and lifetime change of CdSe QDs. It was explained that the thiol head groups act as a hole scavenger. However, for CdTe QDs, fluorescence quenching and lifetime change were not observed.[32] This difference was explained by noting that the reduction potential of aliphatic thiol ligands is located between the valence band edge position of CdSe (*ca.* −6.0 eV *vs* vacuum) and CdTe QDs (*ca.* −5.5 eV *vs* vacuum). The lower energy level of CdSe QDs leads to hole capture, while the higher level of CdTe QDs blocks it. The valence band edge of PbS QDs (*ca.*

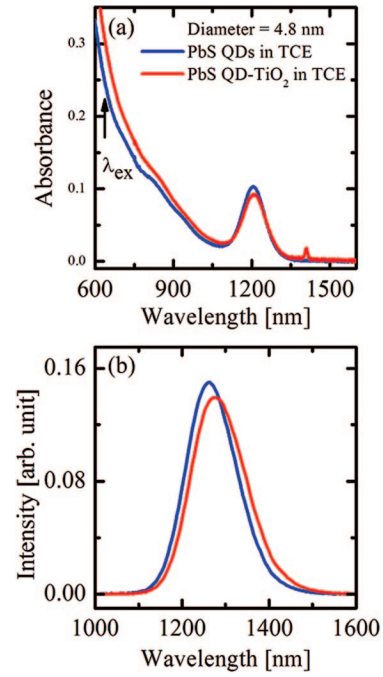

Figure 2. (a) The absorbance and (b) fluorescence spectra of PbS QDs (solid blue lines) of diameter of 4.8 nm and the PbS QD-TiO_2 composite (solid red lines) in tetrachloroethylene (TCE). Fluorescence is measured with 633 nm excitation. The fluorescence spectra were measured under identical conditions, to allow quantitative comparison. The small, sharp peak around 1400 nm in the absorption spectrum of the PbS−TiO_2 composite comes from titanium isopropoxide residue which was not completely hydrolyzed. The TiO_2 is transparent across the indicated range of wavelengths.

−5.0 eV *vs* vacuum) is even higher than that of CdTe QDs as seen Figure 1. Therefore, we expect no change of fluorescence intensity and lifetime of PbS QDs with aliphatic thiol ligands. This was confirmed by comparison of the fluorescence spectra of small and large PbS QDs with and without aliphatic ligands such as 1-decanethiol. Thus, the fluorescence from the PbS-TiO_2 composite is just the intrinsic fluorescence from the thiol-functionalized PbS QDs. Small red shifts of the first exciton absorption peak (~4 nm) and the emission peak (~14 nm) are observed for the PbS−TiO_2 composite. These spectral shifts are not surprising—several prior studies of water-stable QDs wrapped with thiol ligands have reported shifts of the absorption and emission spectra.[33−37] The spectral shift may originate from the redistribution of electronic density and reduction of electron confinement due to the Pb−thiol bond.

Fluorescence transients allow monitoring of the dynamics of the electron population in the QDs. Fluorescence lifetimes in the microsecond range have been reported in prior studies of colloidal lead-salt QDs.[38−40] The fluorescence decay of the PbS−TiO_2 composites with 4.8 nm QDs is identical (within experimental error) to that of the isolated QDs (Figure 3); both have 1.7 μs lifetimes.

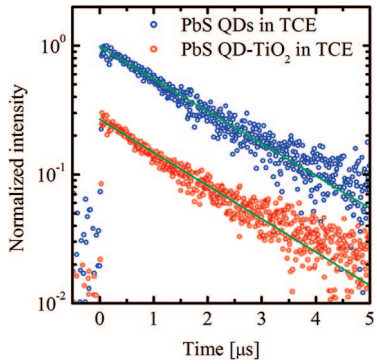

Figure 3. The fluorescence decays of PbS QDs (blue circles) and PbS-TiO_2 composite (red circles) in TCE for PbS QDs with 4.8 nm diameter. Solid green lines: fits to single-exponential decay functions. The details of the fluorescence lifetimes are in the text. For clarity, the fluorescence decay trace of the PbS-TiO_2 is shifted vertically.

The single exponential decay and similar fluorescence lifetime of the composites with the large PbS QDs (diameter >4.3 nm) indicates that the decay dynamics of the composite is dominated by the intrinsic decay dynamics of PbS QDs. This result is consistent with the steady-state fluorescence spectra. Together with the time-integrated fluorescence spectra, these results lead us to conclude that there is negligible transfer of electrons between the 4.8 nm QDs and TiO_2.

For QD diameters less than 4.3 nm coupled to TiO_2 nanoparticles, we would expect to observe evidence of transfer of photoexcited electrons. The absorption spectra of 3.4 nm diameter PbS QDs and PbS QD-TiO_2 composites in TCE are shown in Figure 4a and their fluorescence spectra are in Figure 4b. The lowest absorption peak is broadened, and there is a red-shift of ~36 nm, when the QDs are coupled to the TiO_2. The QD fluorescence is quenched dramatically in the presence of the TiO_2. The quenching is clear despite the increased absorbance of the composite at the excitation wavelength. In addition, the emission peak has shifted to the red by ~35 nm, which is close to the spectral shift of the absorption peak. The strong fluorescence quenching is a signature of electron injection from small PbS QDs into the TiO_2 conduction band.

Fluorescence decays for the 3.4 nm diameter PbS QDs (blue circles in Figure 5) and their PbS QD-TiO_2 composites (red circles in Figure 5) in TCE provide further evidence of electron transfer. The fluorescence of the 3.4 nm diameter PbS QDs decays with a time constant of 4.3 μs (solid green line in Figure 5). The fluorescence decay of the composite is much faster; the emission intensity drops to 10% of the peak value in ~1 μs. The decay is best modeled by a sum of two exponential-decay terms (solid green line), with time constants of 0.11 and 0.81 μs. The average lifetime of the PbS−TiO_2 composite is estimated to be 0.7 μs by use of the expression of intensity-weighted average lifetime, $\langle\tau\rangle = \sum_i a_i\tau_i^2/a_i\tau_i$.[41,42] If we assume that electrons in the QDs decay only by radiative relaxation or

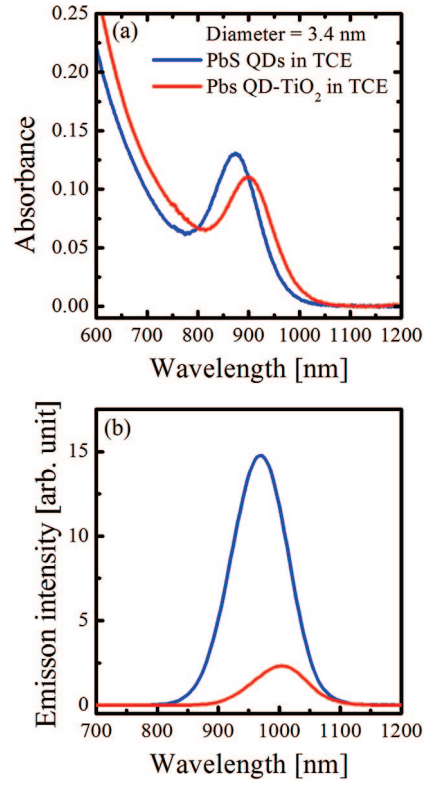

Figure 4. (a) The absorption and (b) fluorescence spectra of 3.4 nm diameter PbS QDs and PbS QD-TiO_2 composites in TCE. Fluorescence is measured with 633 nm excitation.

by transfer to the TiO_2, the electron-transfer rate constant will be $k_{et} = 1/\tau_{(QD+TiO_2)} - 1/\tau_{QD}$.[43] Using the average fluorescence lifetime of the PbS−TiO_2 composite and the intrinsic lifetime of PbS QDs, the electron-transfer rate constant is estimated as 1.19 μs^{-1}, which corresponds to an electron injection time of 0.84 μs. Experiments with 2.9 nm PbS QDs and their PbS QD-TiO2 composites produce similar results, with an electron injection time of 0.45 μs.

To probe charge transfer with greater temporal resolution, femtosecond transient absorption measurements were performed at room temperature with the 3.2 nm diameter PbS QDs and their PbS QD-TiO_2 com-

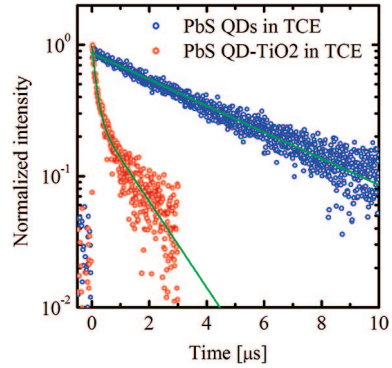

Figure 5. The fluorescence decays of PbS QDs (blue circles) and PbS−TiO_2 composite (red circles) in TCE for PbS QDs with 3.4 nm diameter. Solid green lines: fits using single or double exponential decay functions.

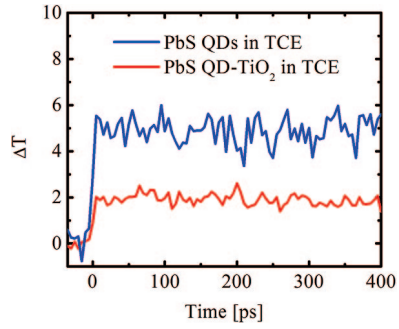

Figure 6. The transient absorption kinetics of PbS QDs (blue line) and PbS QD-TiO2 composites (red line) in TCE for PbS QDs with 3.2 nm diameter. The green solid line is to guide the eye. The samples are excited at a wavelength of 800 nm and probed at 800 nm.

posites (Figure 6). The samples were excited at the first exciton absorption (800 nm) and probed at 800 nm. The transient absorption trace of PbS QDs in TCE shows no change on the time scale of the measurement (a few hundred picoseconds), as expected from the microsecond population decay seen in fluorescence. The transient absorption change of the PbS QD-TiO_2 composite shows the same behavior. There is no fast decay component for these composites. From the results of the transient absorption measurement and fluorescence lifetime, we conclude that the electron transfer time from PbS QDs to TiO_2 nanoparticles in organic solvent is hundreds of nanoseconds.

This electron transfer time is rather slow compared to relevant prior results, and deserves some discussion. The work that is closest to that reported here was done by Plass *et al.*,[18] who synthesized PbS QDs inside porous TiO_2 films, and studied the carrier dynamics with ultrafast transient absorption spectroscopy. These workers monitored the electron population in the QDs, and recorded double-exponential decays. They attribute the longer (~10 ps) time constant to electron transfer, although a detailed model of the dynamics is not presented. A faster (~1 ps) component in the decay is assigned to electron trapping at the interface.

Several factors impede a direct comparison of our work with that of Plass *et al*. First, the materials are not identical: colloidal QDs *versus* QDs grown *in situ*, the presence of the thiol ligands in our work, and amorphous titania in our work *versus* the anatase phase studied by Plass *et al*. We believe that the surface trapping is likely to be reduced in the colloidal samples compared to those grown *in situ*. The colloidal QDs are more monodisperse about the nominal size for each synthesis. Plass and co-workers studied 6 nm PbS QDs, which would not produce any electron transfer to TiO_2 in our experiment. It occurs in their work because they used an organic *p*-type charge transport material and dried TiO_2 nanoparticles, which have a lower electron affinity of −4.45 eV (*vs* vacuum) rather than a liquid electrolyte.

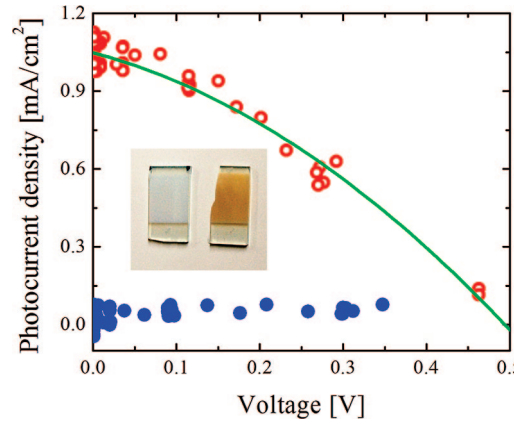

Figure 7. *I*−V characteristic of the PbS QD-sensitized TiO_2 solar cell under 80 mW/cm² illumination (red open circles) and in the dark (blue solid circles). The solid line is to guide the eye. Inset: photos of the titania film before (left) and after (right) incorporation of the QDs.

The electron transfer time that we infer is also much slower than the transfer times inferred similarly from fluorescence quenching in CdSe[13,44] and CdS[45] QD-TiO_2 systems. The energy difference between the LUMO of the QD and the conduction band of TiO_2 is 200 and 400 meV for the 3.4 and 2.9 nm PbS QDs, respectively. CdSe QDs with 7.5 and 4.6 nm diameter have approximately the same energy differences as these PbS QDs when coupled to TiO_2. However, the electron transfer times from CdSe QDs (~0.02 μs for 4.6 nm diameter and 0.12 μs for 7.5 nm diameter)[44] are an order of magnitude faster than those from PbS QDs. It remains to be seen whether the relatively slow electron transfer from PbS QDs will adversely impact the performance of photovoltaic devices. However, we would expect the slow transfer to present a serious impediment to the exploitation of multiple exciton generation, simply because the multiexciton lifetimes will be short compared to the transfer time. It is worth mentioning that the microsecond fluorescence lifetimes of isolated PbS and PbSe QDs[40] are 2 orders of magnitude longer than the lifetimes of CdS and CdSe QDs. Resonant energy transfer is similarly slowed in PbS QDs.[40] We conjecture that the slow electron transfer is an inherent property of lead-salt QDs. Clearly, the relevant physical mechanisms are not understood and much more work is needed on this interesting and important question.

We fabricated prototype Gratzel cells with PbS QDs as the sensitizer. PbS QDs with diameter of 2.9 nm (energy gap ~1.5 eV) were synthesized with the linker molecule described above. Films of 25 nm TiO_2 particles with thickness ranging from 2 to 8 μm were deposited on fluorinated tin oxide electrodes. (Details of the fabrication are in the Supporting Information.) The QDs were infiltrated into the TiO_2 films, and the I^-/I_3^- electrolyte commonly used as the redox couple for ruthenium dyes completed the cells. Strong scattering from the films made it difficult to quantitatively assess the concentration of QDs *via* the absorption spectrum. The

photocurrent−voltage curve for a cell with 4 μm thick titania is shown in Figure 7 as an example. The open-circuit voltage, short-circuit current density, fill factor, and energy conversion efficiency of this cell are 0.49 V, 1 mA/cm,^{2} 57%, and 0.28%, respectively. These results confirm the role of the QDs in efficiently sensitizing the titania. Considering that no attempt was made to optimize the performance, the results are encouraging, and we expect that significant improvement can be made. Practical issues such as potential instability of lead-salt QDs in the iodide electrolyte will have to be addressed.

CONCLUSION

The energy levels (relative to vacuum) of electrons in PbS QDs have been determined through cyclic voltammetry, and the results agree well with calculations that account for quantum confinement of the electrons and the dielectric properties of the QDs. The results imply a favorable energetic pathway for electron injection into TiO_2 nanoparticles in organic solvents for QD diameters below 4.3 nm. Small PbS QDs coupled to TiO_2 nanoparticles exhibit strong fluorescence quenching and rapid fluorescence decays, which are consistent with efficient electron transfer to the TiO_2. Analogous studies can easily be performed for other metal oxide electrode materials. We believe that further work will be needed to quantify the rate of electron injection from lead-salt QDs, and such work is now being planned. Finally, nanoscale titania films were successfully sensitized with the colloidal PbS QDs of appropriate size. These results will guide the future development of solar cells sensitized by PbS QDs, which are strong candidates to exploit possible carrier multiplication in QDs.

EXPERIMENTAL DETAILS

TiO_2 nanoparticles were synthesized according to the approach of Robel *et al.*[13] Colloidal PbS QDs were assembled to the TiO_2 nanoparticles by bifunctional linker molecules with 3-mercaptopropionic acid (MPA). Details of the syntheses are in the Supporting Information. Absorption spectra were measured at room temperature. Emission spectra were recorded at room temperature with an infrared fluorometer equipped with a 200 mm focal length monochromator, a 25 mW HeNe laser as the excitation source, and an InGaAs photodiode. For time-resolved fluorescence and transient absorption measurements, the samples were excited at a repetition rate of 1 kHz by femtosecond pulses at 800 nm. For time-resolved fluorescence measurements, the ultrashort pulse duration is not needed; this was used only for convenience. The sample was exposed to microwatt average power levels so that the excitation level was always well below one electron−hole pair per dot. Fluorescence was monitored with a 125 MHz InGaAs photoreceiver. The output was fed into a digital oscilloscope and averaged, which provides an instrument response of a few nanoseconds and adequate dynamic range to monitor decay times in the microsecond range.

Acknowledgment. The research described here was partially supported by the Center for Nanoscale Systems through National Science Foundation Grant No. EEC-0646547 and by NYSTAR.

Supporting Information Available: Description of synthesis and surface modification of TiO_2 nanoparticles, cyclic voltammetric analysis, and fabrication of solar cells. This material is available free of charge *via* the Internet at http://pubs.acs.org.

REFERENCES AND NOTES

1. Ross, R. T.; Nozik, A. J. Efficiency of Hot-Carrier Solar-Energy Converters. *J. Appl. Phys.* **1982**, *53*, 3813–3818.
2. Nozik, A. J. Spectroscopy and Hot Electron Relaxation Dynamics in Semiconductor Quantum Wells and Quantum Dots. *Annu. Rev. Phys. Chem.* **2001**, *52*, 193–231.
3. Nozik, A. J. Quantum Dot Solar Cells. *Phys. E* **2002**, *14*, 115–120.
4. Luque, A.; Mart, A. Increasing the Efficiency of Ideal Solar Cells by Photon Induced Transitions at Intermediate Levels. *Phys. Rev. Lett.* **1997**, *78*, 5014–5017.
5. Greenham, N. C.; Peng, X.; Alivisatos, A. P. Charge Separation and Transport in Conjugated-Polymer/Semiconductor-Nanocrystal Composites Studied by Photoluminescence Quenching and Photoconductivity. *Phys. Rev. B* **1996**, *54*, 17628–17637.
6. Green, M. A. Third Generation Photovoltaics: Solar Cells for 2020 and Beyond. *Phys. E* **2002**, *14*, 65–70.
7. Nazeeruddin, M. K.; Pechy, P.; Renouard, T.; Zakeeruddin, S. M.; Humphry-Baker, R.; Comte, P.; Liska, P.; Cevey, L.; Costa, E.; Shklover, V.; *et al.* M. Engineering of Efficient Panchromatic Sensitizers for Nanocrystalline TiO_2-based Solar Cells. *J. Am. Chem. Soc.* **2001**, *123*, 1613–1624.
8. Gerischer, H.; Lubke, M. A Particle-Size Effect in the Sensitization of TiO_2 Electrodes by a CdS Deposit. *J. Electroanal. Chem.* **1986**, *204*, 225–227.
9. Nasr, C.; Hotchandani, S.; Kim, W. Y.; Schmehl, R. H.; Kamat, P. V. Photoelectrochemistry of Composite Semiconductor Thin Films. Photosensitization of SnO_2/CdS Coupled Nanocrystallites with A Ruthenium Polypyridyl Complex. *J. Phys. Chem. B* **1997**, *101*, 7480–7487.
10. Hao, E. C.; Yang, B.; Zhang, J. H.; Zhang, X.; Sun, J. Q.; Shen, S. C. Assembly of Alternating TiO_2/CdS Nanoparticle Composite Films. *J. Mater. Chem.* **1998**, *8*, 1327–1328.
11. Lawless, D.; Kapoor, S.; Meisel, D. Bifunctional Capping of CDS Nanoparticle and Bridging to TIO_2. *J. Phys. Chem.* **1995**, *99*, 10329–10335.
12. Nasr, C.; Kamat, P. V.; Hotchandani, S. Photoelectrochemical Behavior of Coupled SnO_2 Vertical Bar CdSe Nanocrystalline Semiconductor Films. *J. Electroanal. Chem.* **1997**, *420*, 201–207.
13. Robel, I.; Subramanian, V.; Kuno, M.; Kamat, P. V. Quantum Dot Solar Cells. Harvesting Light Energy with CdSe Nanocrystals Molecularly Linked to Mesoscopic TiO_2 Films. *J. Am. Chem. Soc.* **2006**, *128*, 2385–2393.
14. Zaban, A.; Micic, O. I.; Gregg, B. A.; Nozik, A. J. Relative Energetics at the Semiconductor/Sensitizing Dye/Electrolyte Interface. *Langmuir* **1998**, *14*, 3153–3156.
15. Yu, P. R.; Zhu, K.; Norman, A. G.; Ferrere, S.; Frank, A. J.; Nozik, A. J. Nanocrystalline TiO_2 Solar Cells Sensitized with InAs Quantum Dots. *J. Phys. Chem. B* **2006**, *110*, 25451–25454.
16. Vogel, R.; Hoyer, P.; Weller, H. Quantum-Sized PbS, CdS, Ag_2S, Sb_2S_3, and Bi_2S_3 Particles as Sensitizers for Various Nanoporous Wide-Bandgap Semiconductors. *J. Phys. Chem.* **1994**, *98*, 3183–3188.
17. Hoyer, P.; Konenkamp, R. Photoconduction in Porous TiO_2 Sensitized by PbS Quantum Dots. *Appl. Phys. Lett.* **1995**, *66*, 349–351.
18. Plass, R.; Pelet, S.; Krueger, J.; Gratzel, M.; Bach, U. Quantum Dot Sensitization of Organic-Inorganic Hybrid Solar Cells. *J. Phys. Chem. B* **2002**, *106*, 7578–7580.
19. Wise, F. W. Lead Salt Quantum Dots: The Limit of Strong Quantum Confinement. *Acc. Chem. Res.* **2000**, *33*, 773–780.

20. Schaller, R. D.; Sykora, M.; Pietryga, J. M.; Klimov, V. I. Seven Excitons at a Cost of One: Redefining the Limits for Conversion Efficiency of Photons into Charge Carriers. *Nano Lett.* **2006**, *6*, 424–429.
21. Hines, M. A.; Scholes, G. D. Colloidal PbS Nanocrystals with Size-Tunable Near-Infrared Emission: Observation of Post-Synthesis Self-Narrowing of the Particle Size Distribution. *Adv. Mater.* **2003**, *15*, 1844–1849.
22. Konstantatos, G.; Clifford, J.; Levina, L.; Sargent, E. H. Sensitive Solution-Processed Visible-Wavelength Photodetectors. *Nat. Photonics* **2007**, *1*, 531–534.
23. Murray, C. B.; Sun, S.; Gaschler, W.; Doyle, H.; Betley, T. A.; Kagan, C. R. Colloidal Synthesis of Nanocrystals and Nanocrystal Superlattices. *IBM J. Res. Dev.* **2001**, *45*, 47–56.
24. Kang, I.; Wise, F. W. Electronic Structure and Optical Properties of PbS and PbSe Quantum Dots. *J. Opt. Soc. Am., B* **1997**, *14*, 1632–1646.
25. Jiang, X. M.; Schaller, R. D.; Lee, S. B.; Pietryga, J. M.; Klimov, V. I.; Zakhidov, A. A. PbSe Nanocrystal/Conducting Polymer Solar Cells with an Infrared Response to 2 Micron. *J. Mater. Res.* **2007**, *22*, 2204–2210.
26. Brus, L. E. A Simple Model for the Ionization Potential, Electron Affinity, and Aqueous Redox Potentials of Small Semiconductor Crystallites. *J. Chem. Phys.* **1983**, *79*, 5566–71.
27. Moreels, L.; Lambert, K.; De Muynck, D.; Vanhaecke, F.; Poelman, D.; Martins, J. C.; Allan, G.; Hens, Z. Composition and Size-Dependent Extinction Coefficient of Colloidal PbSe Quantum Dots. *Chem. Mater.* **2007**, *19*, 6101–6106.
28. Guizzett, G.; Filippin, F.; Reguzzon, E.; Samoggia, G. Electrical Properties and Spectral Response of PbS−Ge Heterojunctions. *Phys. Status Solidi A* **1971**, *6*, 605–610.
29. Knapp, R. A. Photoelectric Properties of Lead Sulfide in the Near and Vacuum Ultraviolet. *Phys. Rev.* **1963**, *132*, 1891–1897.
30. Wei, S. H.; Zunger, A. Electronic and Structural Anomalies in Lead Chalcogenides. *Phys. Rev. B* **1997**, *55*, 13605–13610.
31. Cahen, D.; Hodes, G.; Gratzel, M.; Guillemoles, J. F.; Riess, I. Nature of Photovoltaic Action in Dye-Sensitized Solar Cells. *J. Phys. Chem. B* **2000**, *104*, 2053–9.
32. Wuister, S. F.; deMelloDonega, C.; Meijerink, A. Influence of Thiol Capping on the Exciton Luminescence and Decay Kinetics of CdTe and CdSe Quantum Dots. *J. Phys. Chem. B* **2004**, *108*, 17393–17397.
33. Wuister, S. F.; Swart, I.; van Driel, F.; Hickey, S. G.; Donega, C. D. Highly Luminescent Water-Soluble CdTe Quantum Dots. *Nano Lett.* **2003**, *3*, 503–507.
34. Wuister, S. F.; Donega, C. D.; Meijerink, A. Local-Field Effects on the Spontaneous Emission Rate of CdTe and CdSe Quantum Dots in Dielectric Media. *J. Chem. Phys.* **2004**, *121*, 4310–4315.
35. Zhelev, Z.; Bakalova, R.; Ohba, H.; Jose, R.; Imai, Y.; Baba, Y. Uncoated, Broad Fluorescent, and Size-Homogeneous CdSe Quantum Dots for Bioanalyses. *Anal. Chem.* **2006**, *78*, 321–330.
36. Gerion, D.; Pinaud, F.; Williams, S. C.; Parak, W. J.; Zanchet, D.; Weiss, S.; Alivisatos, A. P. Synthesis and Properties of Biocompatible Water-Soluble Silica-Coated CdSe/ZnS Semiconductor Quantum Dots. *J. Phys. Chem. B* **2001**, *105*, 8861–8871.
37. Hyun, B. R.; Chen, H. Y.; Rey, D. A.; Wise, F. W.; Batt, C. A. Near-Infrared Fluorescence Imaging with Water-Soluble Lead Salt Quantum Dots. *J. Phys. Chem. B* **2007**, *111*, 5726–5730.
38. Du, H.; Chen, C. L.; Krishnan, R.; Krauss, T. D.; Harbold, J. M.; Wise, F. W.; Thomas, M. G.; Silcox, J. Optical Properties of Colloidal PbSe Nanocrystals. *Nano Lett.* **2002**, *2*, 1321–1324.
39. Wehrenberg, B. L.; Wang, C. J.; Guyot-Sionnest, P. Interband and Intraband Optical Studies of PbSe Colloidal Quantum Dots. *J. Phys. Chem. B* **2002**, *106*, 10634–10640.
40. Clark, S. W.; Harbold, J. M.; Wise, F. W. Resonant Energy Transfer in PbS Quantum dots. *J. Phys. Chem. C* **2007**, *111*, 7302–7305.
41. James, D. R.; Liu, Y. S.; Demayo, P.; Ware, W. R. Distributions of Fluorescence Lifetimes—Consequences for the Photophysics of Molecules Adsorbed on Surfaces. *Chem. Phys. Lett.* **1985**, *120*, 460–465.
42. Lakowicz, J. R. *Principles of Fluorescence Spectroscoy*, 2nd ed; Plenum: New York, 1999.
43. Kamat, P. V.; Chauvet, J. P.; Fessenden, R. W. Photoelectrochemistry in Particulate Systems 0.4. Photosensitization of a TiO_2 Semiconductor with a Chlorophyll Analog. *J. Phys. Chem.* **1986**, *90*, 1389–1394.
44. Robel, I.; Kuno, M.; Kamat, P. V. Size-Dependent Electron Injection from Excited CdSe Quantum Dots into TiO_2 Nanoparticles. *J. Am. Chem. Soc.* **2007**, *129*, 4136–4137.
45. Blackburn, J. L.; Selmarten, D. C.; Nozik, A. J. Electron Transfer Dynamics in Quantum Dot/Titanium Dioxide Composites Formed by *in Situ* Chemical Bath Deposition. *J. Phys. Chem. B* **2003**, *107*, 14154–14157.